MODELLING SOLAR IRRADIANCE VARIATIONS: SEPARATE MODELS FOR THE NETWORK AND ACTIVE REGION FACULAE

T. Wenzler[1], S.K. Solanki[2], D.M. Fluri[1], C. Frutiger[1], M. Fligge[1], and A. Ortiz[3]

[1]Institute of Astronomy, ETH-Zentrum, 8092 Zurich, Switzerland (wenzler@astro.phys.ethz.ch)
[2]Max-Planck-Institut für Aeronomie, 37191 Katlenburg-Lindau, Germany (solanki@linmpi.mpg.de)
[3]Dept. Astronomia i Meteorologia, Universitat de Barcelona, 08028 Barcelona, Spain (aortiz@am.ub.es)

ABSTRACT

In order to determine to what extent solar surface magnetism affects solar irradiance we need to reconstruct the irradiance from magnetograms. This process requires the use of model atmospheres. Here we present two model atmospheres describing faculae in active regions and the network. The models have been constructed such that they reproduce various data sets simultaneously.

Key words: solar activity; irradiance variations; faculae; network.

1. INTRODUCTION

The final aim of the current project is to calculate solar irradiance variations making use of plane-parallel 1-component model atmospheres representing quiet Sun, sunspot, network, and facular regions. Although sunspot and quiet Sun models of good quality are available, there is still considerable room for improvement for models of faculae and the network. We distinguish between faculae and the network by the spatially averaged field strength, with faculae being associated with large and the network with smaller spatially averaged field strength. For example, previous reconstructions (e.g. Fligge et al. 2000a,b) used only a single model (constructed by Unruh et al. 1999) to describe both these components. There is, however, mounting evidence that the thermal and radiative properties of the flux tubes underlying these features are different (Solanki & Stenflo 1984; Solanki 1986; Topka et al. 1997; Ortiz et al. 2000). In this work we present separate network and facular models based on contrast and flux observations. In order to calculate fluxes, intensities and contrasts of each of these components, we employ the Kurucz's ATLAS9 spectral synthesis code (Kurucz 1992a,b,c) that takes into account up to 58 million lines by means of opacity distribution functions. We neglect non-LTE effects.

2. THE 3-COMPONENT MODEL (PREVIOUS WORK)

Fligge et al. (2000a,b) have reconstructed the solar irradiance variations based on a 3-component model describing quiet Sun, sunspots, and faculae. The surface distribution of the solar magnetic field is extracted from full-disk magnetograms obtained by the Michelson Doppler Interferometer (MDI) onboard the Solar and Heliospheric Observatory (SOHO) of ESA and NASA. In the following we present first steps towards the modelling of facular regions.

3. CONTRAST OBSERVATIONS

MDI observations by Ortiz et al. (2000) (cf. Topka et al. 1997) show that the centre-to-limb variation (CLV) of the facular contrast relative to the quiet Sun depends on the magnetic flux per pixel (see Figure 1).

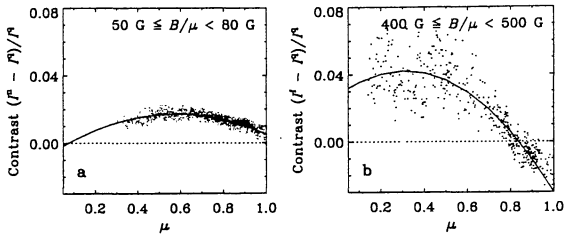

Figure 1. Contrast as a function of μ for two different bins of B/μ (Ortiz et al. 2000). A second order polynomial has been fitted to the data (solid curve). I^q, I^n, and I^f are the intensities of the quiet Sun, network, and the faculae, respectively. **a** *Contrast of features with low magnetic flux per pixel (network).* **b** *Contrast of features with high magnetic flux per pixel (faculae).*

Therefore, facular regions should be described by

Proc. SOHO 11 Symposium, 'From Solar Min to Max: Half a Solar Cycle with SOHO', Davos, Switzerland, 11-15 March 2002 (ESA SP-508, June 2002)

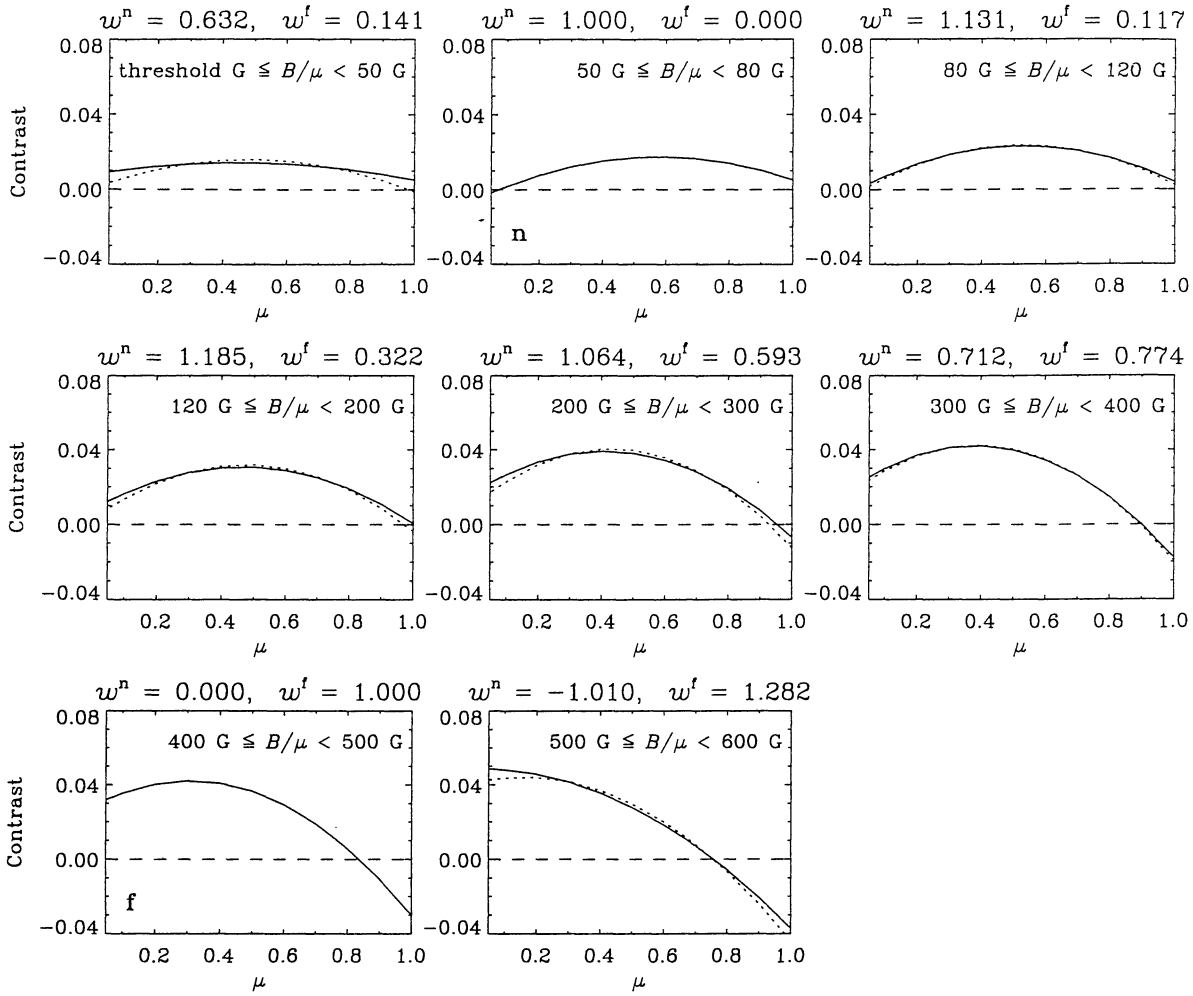

Figure 2. Contrast as a function of μ for eight different bins of B/μ (Ortiz et al. 2000). We have only plotted the second order polynomial that has been fitted to the observed data (solid curve). The dotted curve shows the linear combination of the network (n) and the facular (f) data.

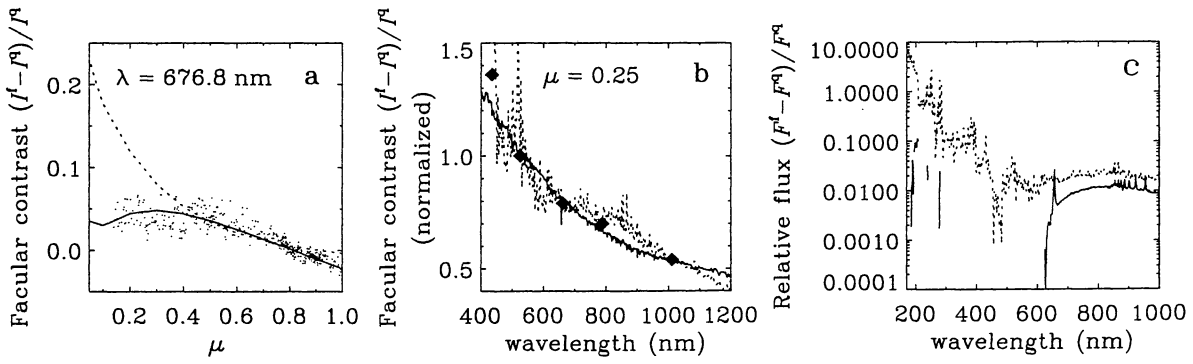

Figure 3. Facular contrast vs. μ (panel a), facular contrast normalized to its value at 525 nm vs. wavelength (panel b), and relative flux vs. wavelength (panel c) of two facular models (solid and dotted curves). One model (solid) fits well the contrast observations but fails to produce a reasonable UV flux. The second model deviates from the CLV of the contrast near the limb, but produces a more reasonable UV spectrum. Both models reproduce the wavelength dependence of the contrast. As a compromise we employ the second model (dotted) in the following.

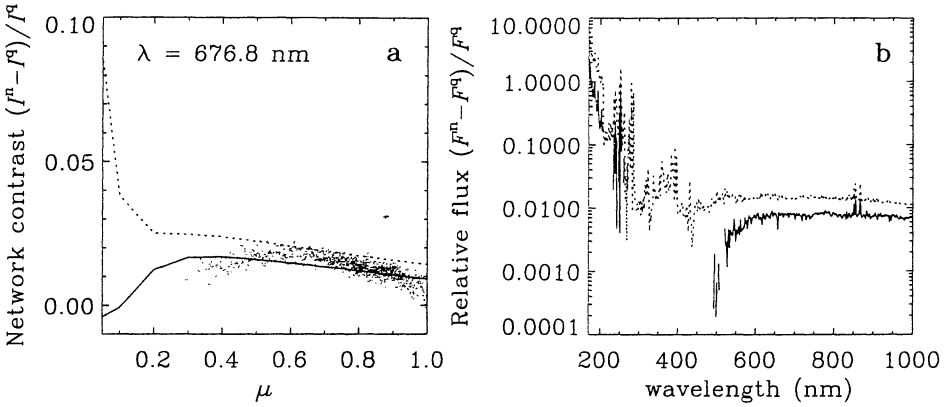

Figure 4. Network contrast vs. μ (panel a) and relative flux vs. wavelength (panel b) of two network models (solid and dotted curves). Again a reasonable UV flux is only obtained when increasing the contrast considerably for small μ (dotted curve).

multiple model atmospheres. We construct two facular models, one describing the network (Figure 1a), the other describing active region faculae (Figure 1b). The distinction is actually between regions with low and high spatially averaged field strength, but we refer to them as network and active region faculae for simplicity. The CLV of faculae with B/μ values outside the ranges given in Figure 1 can be represented by a linear combination of these two models

$$c(B/\mu) = w^{\rm n}(B/\mu)\cdot c^{\rm n} + w^{\rm f}(B/\mu)\cdot c^{\rm f}\,, \qquad (1)$$

where c is the contrast relative to the quiet Sun, B is the magnetogram signal, $\mu = \cos(\theta)$ is the heliocentric angle, and w is a weighting factor. The superscript 'n' stands for network and 'f' for faculae (see Figure 2).

4. FACULAR MODEL

The facular model is constrained to reproduce the CLV of the contrast (dots in Figure 1b and Figure 3a) observed by Ortiz et al. (2000) plus the spectral variation of the contrast near $\mu = 0.25$ (diamonds in Figure 3b) observed by Chapman & McGuire (1977).

In Figure 3 we give the contrast and the relative flux of two possible facular models. The model atmosphere (solid) that fits the observed contrast well fails to produce a reasonable UV flux. To obtain a more realistic flux we choose the second model (dotted) to describe faculae in the following although we had to increase the contrast near the limb.

5. NETWORK MODEL

The network model is required to reproduce the CLV of the contrast (dots in Figure 1a and Figure 4a) observed by Ortiz et al. (2000). The data of Chapman & McGuire (1977) refers to strong faculae and has therefore not been employed to constrain the network model.

We see in Figure 4 that a large enough UV flux is only produced with a high contrast close to the limb. Therefore, we employ the atmosphere corresponding to the dotted curves in Figure 4 as the network model. Note that the contrast at $\mu < 0.3$ is not constrained by the MDI data for the low field case (no data points above the noise).

6. RELATIVE FLUX VARIATIONS

The relative flux (or relative irradiance) variations between solar-activity maximum and minimum as a function of wavelength can be written as

$$\frac{\Delta F_\lambda}{F^{\rm q}_\lambda} = \frac{(1-\alpha^{\rm f}-\alpha^{\rm n}-\alpha^{\rm s})F^{\rm q}_\lambda}{F^{\rm q}_\lambda} + \frac{\alpha^{\rm f}F^{\rm f}_\lambda + \alpha^{\rm n}F^{\rm n}_\lambda + \alpha^{\rm s}F^{\rm s}_\lambda - F^{\rm q}_\lambda}{F^{\rm q}_\lambda}\,, \qquad (2)$$

with F^i_λ, $i \in \{{\rm q,f,n,s}\}$ being the fluxes of the four different model atmospheres. To derive Equation 2 we assume that during the activity minimum the flux can be described by the quiet Sun model atmosphere.

The relative flux variations are given in Figure 5. The dotted curve shows the UV data as compiled by Lean (1997) for wavelengths smaller than 400 nm. The solid curve is our 4-component model fit (see Equation 2), assuming a global facular filling factor of $\alpha^{\rm f} = 4\%$, a network filling factor of $\alpha^{\rm n} = 8\%$ and a spot filling factor of $\alpha^{\rm s} = 0.23\%$. With these global filling factors the total irradiance variation

$$\frac{\Delta F^{\rm tot}}{F^{\rm tot}} = \frac{\int \Delta F_\lambda\, d\lambda}{\int F^{\rm q}_\lambda\, d\lambda} \qquad (3)$$

comes out to be 0.1 %, which is consistent with the Active Cavity Radiometer Irradiance Monitor

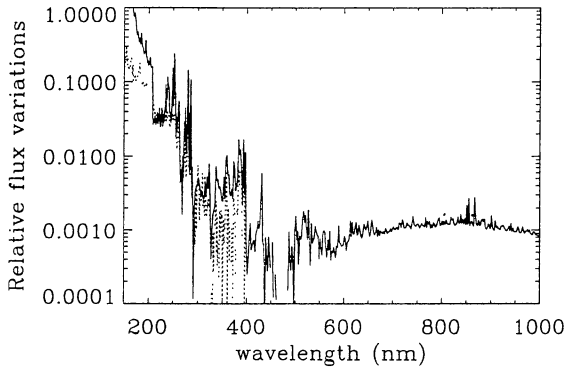

Figure 5. Relative flux (or relative irradiance) variations over the solar cycle vs. wavelength. The dotted curve represents observations (Lean 1997) for wavelengths shorter than 400 nm. The solid curve shows the relative irradiance variations resulting from a 4-component model with global filling factors at maximum of 4% (faculae), 8% (network), and 0.23% (spots). The total irradiance variation predicted by the model is 0.1%. We have used the facular and network models producing the dotted curves in Figure 3 and Figure 4.

(ACRIM, Willson & Hudson 1991) and the Earth Radiation Budget (ERB, Kyle et al. 1994) measurements.

7. DISCUSSION

We have shown that the network and the facular model atmospheres can, within limits, reproduce various data sets simultaneously. In particular, our model can reproduce the relative flux variations between maximum and minimum of the solar activity cycle with a reasonable choice of filling factors. This supports the idea that the irradiance variations are mainly caused by magnetic fields at the solar surface.

We find, however, that it is impossible to model the near-limb behavior of the contrast together with the strong increase of the flux in the UV. This might be due to the fact that our plane-parallel 1-component models neglect the geometry of the magnetic elements. A consistent treatment of flux tubes (which are the basic magnetic structures underlying network and active region faculae) would naturally lead to a decreasing contrast of faculae towards the limb because of the decreasing visibility of the hot wall there (Spruit 1976).

Next generation models need to incorporate flux tube physics in order to simultaneously reproduce the CLV of the contrast and the UV spectral variation. In addition, there is a need of further observations to constrain the upper photospheric layers of the models better.

REFERENCES

Chapman G.A., McGuire T.E., 1977, ApJ, 217, 657

Fligge M., Solanki S.K., Meunier N., Unruh Y.C., 2000a, ESA, SP-463, 117

Fligge M., Solanki S.K., Unruh Y.C., 2000b, A&A, 353, 380

Kurucz R.L., 1992a, Rev. Mex. Astron. Astrofis., 23, 45

Kurucz R.L., 1992b, Rev. Mex. Astron. Astrofis., 23, 181

Kurucz R.L., 1992c, Rev. Mex. Astron. Astrofis., 23, 187

Kyle H.L., Hoyt D.V., Hickey J.R., 1994, Sol. Phys., 152, 9

Lean J., 1997, ARA&A, 35, 33

Ortiz A., Solanki S.K., Fligge M., Domingo V., Sanahuja B., 2000, ESA, SP-463, 399

Solanki S.K., 1986, A&A, 168, 311

Solanki S.K., Stenflo J.O., 1984, A&A, 140, 185

Spruit H.C., 1976, Sol. Phys., 50, 269

Topka K.P., Tarbell T.D., Title A.M., 1997, ApJ, 484, 479

Unruh Y.C., Solanki S.K., Fligge M., 1999, A&A, 345, 635

Willson R.C., Hudson H.S., 1991, Nat, 351, 42